

Cooling the skin for assessing small-fibre function

Leone, C; Dufour, A; Di Stefano, G; Fasolino, A; Di Lionardo, A; La Cesa, S; Galosi, E; Valeriani, M; Nolano, M; Cruccu, G; Truini, A

Published in:
Pain

DOI (link to publication from Publisher):
[10.1097/j.pain.0000000000001584](https://doi.org/10.1097/j.pain.0000000000001584)

Publication date:
2019

Document Version
Accepted author manuscript, peer reviewed version

[Link to publication from Aalborg University](#)

Citation for published version (APA):

Leone, C., Dufour, A., Di Stefano, G., Fasolino, A., Di Lionardo, A., La Cesa, S., Galosi, E., Valeriani, M., Nolano, M., Cruccu, G., & Truini, A. (2019). Cooling the skin for assessing small-fibre function. *Pain*, 160(9), 1967-1975. <https://doi.org/10.1097/j.pain.0000000000001584>

General rights

Copyright and moral rights for the publications made accessible in the public portal are retained by the authors and/or other copyright owners and it is a condition of accessing publications that users recognise and abide by the legal requirements associated with these rights.

- Users may download and print one copy of any publication from the public portal for the purpose of private study or research.
- You may not further distribute the material or use it for any profit-making activity or commercial gain
- You may freely distribute the URL identifying the publication in the public portal -

Take down policy

If you believe that this document breaches copyright please contact us at vbn@aub.aau.dk providing details, and we will remove access to the work immediately and investigate your claim.

Cooling the skin for assessing small-fibre function

C Leone¹, A Dufour², G Di Stefano¹, A Fasolino¹, A Di Lionardo¹, S La Cesa¹, E Galosi¹, M Valeriani^{3,4}, M Nolano⁵, G Cruccu¹, A Truini¹

¹. Department of Human Neuroscience, Sapienza University, Rome, Italy

². Centre d'Investigations Neurocognitives et Neurophysiologiques (CI2N), CNRS, University of Strasbourg, France.

³. Center for Sensory-Motor Interaction, Aalborg University, Denmark

⁴. Ospedale Bambino Gesù, IRCCS, Rome, Italy.

⁵. "Salvatore Maugeri" Foundation, Institute of Telesse Terme (BN), Telesse Terme (BN), Italy

Corresponding Author

Andrea Truini, Department of Human Neuroscience, Sapienza University, Viale Università 30, 00185 - Rome, Italy (andrea.truini@uniroma1.it)

Abstract

In this clinical and neurophysiological study using a novel cold stimulator we aim at investigating whether cold evoked potentials may prove to be a reliable diagnostic tool to assess trigeminal small-fibre function.

Using a novel device consisting of micro-Peltier elements, we recorded cold evoked potentials after stimulating the supraorbital and perioral regions and the hand dorsum in 15 healthy participants and in two patients with exemplary facial neuropathic pain conditions. We measured peripheral conduction velocity at the upper arm and studied the brain generators using source analysis. In healthy participants and patients, we also compared cold evoked potentials with laser evoked potentials.

In the healthy participants, cold stimulation evoked reproducible scalp potentials, similar to those elicited by laser pulses, though with a latency of about 30 ms longer. The mean peripheral conduction velocity, estimated at the upper arm, was 12.7 m/s. The main waves of the scalp potentials originated from the anterior cingulate gyrus and were preceded by activity in the bilateral opercular regions and bilateral dorso-lateral frontal regions. Unlike laser stimulation, cold stimulation evoked scalp potential of similar amplitude across perioral, supraorbital and hand dorsum stimulation. In patients with facial neuropathic pain, cold evoked potential recording showed the selective damage of cold pathways providing complementary information to laser evoked potential recording.

Our clinical and neurophysiological study shows that this new device provides reliable information on trigeminal small-fibres mediating cold sensation, and might be useful for investigating patients with facial neuropathic pain associated with a distinct damage of cold-mediating fibres.

Keywords: cold, small-fibre neuropathy, neuropathic pain, central pain

Introduction

The current neurophysiological assessment of trigeminal small-fibre function relies on recording of heat-mediated evoked potentials, i.e. laser evoked potentials and contact heat-evoked potentials [7,32,38, 2]. Although these two techniques are widely used to assess trigeminal small-fibre function, for clinical and experimental purposes, they do not provide any information on small-nerve fibres that mediate cold sensations. Nevertheless, several studies have shown that abnormalities in cold-mediating fibres are distinctly involved in different neuropathic pain conditions, such as idiopathic trigeminal neuropathy and central post-stroke pain [28; 4,19].

A new tool based on micro-Peltier elements, able to produce steep cooling ramps of up to -300°C/s , has recently been devised. This tool, providing rapid and painless skin cooling, elicits cold evoked potentials (CEPs) at latencies compatible with A δ -fibre conduction velocity [6]. Therefore, recording CEPs may complement laser evoked potentials in assessing small-fibre function in patients with neuropathic pain. Having more information on trigeminal cold-mediating fibre function might be useful to improve our knowledge on the different trigeminal neuropathic pain conditions.

The aim of this clinical and neurophysiological study was to test the clinical usefulness of this new tool for assessing trigeminal cold-mediating fibres. To do so, we compared CEPs and laser evoked potentials, investigated the cerebral dipole sources of CEPs in 15 healthy participants and verified how precise CEPs are in revealing selective cold-mediating fibre damage in two patients with exemplary trigeminal neuropathic pain conditions.

Methods

Study cohort

We consecutively enrolled 15 healthy participants from among the hospital personnel (8F; 7M; age 25.6 ± 3) and two patients with facial neuropathic pain. Patient 1, a man aged 78 years, was suffering from idiopathic trigeminal neuropathy [4]. This patient complained of ongoing pain, tingling sensations and touch and cold hypoesthesia. Patient 2, a man aged 65 years, suffered from central post-stroke pain resulting from a previous haemorrhagic stroke in the right thalamic region. This patient complained of left-side thermal-pain hypoesthesia, ongoing pain and cold allodynia involving the face and the hand.

Each healthy participant underwent laser and cold stimulation during the same experimental session. We stimulated the right side above the eyebrow, the perioral region and the hand dorsum. The order of the laser and cold stimulation and the stimulated areas were randomly alternated across the different participants. In the patient with idiopathic trigeminal neuropathy, we stimulated the perioral region of the right side (given that this condition affects the trigeminal nerve bilaterally and, in this patient, the sensory disturbances were symmetrically distributed on both sides). In the patient with central post-stroke pain, we stimulated the perioral region of the affected and normal side. The two patients underwent quantitative sensory testing and laser evoked potentials related to A δ -fibres. The patient with idiopathic trigeminal neuropathy also underwent skin biopsy and laser evoked potentials related to C-fibres. In this patient, we used these two techniques to identify the sparing of C-fibres, a distinctive feature of trigeminal neuropathy [4]. The study was approved by the local Institutional Review Board.

Cold stimulation

Subjects were asked to lie down comfortably on a medical cot. We stimulated the skin over the right supraorbital, perioral regions and hand dorsum with a new cold stimulator (QST.Lab, Strasbourg, France). This stimulation probe has a flat surface area of 160 mm^2 consisting of 16 embedded micro-Peltier elements. Micro-Peltier elements have a surface area of 7.7 mm^2 and the central micro-Peltier element has a surface area of 2 mm^2 . A thermocouple located at the centre of the stimulation surface drives the micro-Peltier elements at a frequency of 1000 Hz. Since the thermocouple is embedded in the solder of the central micro-Peltier, the influence of skin temperature is negligible, i.e. 0.1°C for a stimulation temperature of 20°C below skin temperature. The stimulation cools the skin with ramps of up to -300°C/s . The neutral skin temperature for each subject was identified directly by the stimulation probe. We set the stimulation probe to elicit cold stimulation with 10°C as a target temperature [6]. The stimulus duration was 500 ms. Care was taken throughout the session to maintain good contact between the probe and the subject's skin. We delivered 30 stimuli to the supraorbital, perioral region and hand dorsum. During the experiment, the stimulation probe was shifted slightly after each stimulus and the interstimulus interval (10–15 s) was varied randomly. Each subject was asked to rate the cold sensation using a 0–10 numeric rating scale (NRS), where 0 corresponded to no sensation and 10 to the coldest imaginable sensation.

In five subjects we stimulated the hand, the forearm and the shoulder (with a fixed distance of 20 cm) to estimate the conduction velocity of cold-mediating fibres.

Laser stimulation

Subjects were asked to lie down on a medical cot and wore protective eye goggles. We stimulated the skin of the right supraorbital and perioral regions and hand dorsum with a Neodymium-YAP stimulator (ELEN, Florence, Italy). Laser pulses were set at relatively high intensity (stimuli 89-115 mJ/mm²), short duration (5 ms) and a small diameter (5 mm), eliciting a clear painful pinprick sensation, mediated by A δ afferents, and producing a subjective rating of at least 4 on a 0–10 numeric rating scale (NRS) (0 = no sensation, 10 = worst possible pain). We delivered 15 stimuli to each stimulation site. To avoid skin burns, nociceptor fatigue and central habituation, the laser beam was shifted slightly after each stimulus and the interstimulus interval (10–15 s) was varied randomly. Each subject rated the pinprick sensation using a 0–10 numeric rating scale (NRS).

EEG recordings

The EEG was recorded using 32 actively shielded Ag-AgCl electrodes mounted in an elastic electrode cap and arranged according to the International 10-20 system. The EEG recordings were analysed offline using LetsWave 6 (<http://www.nocions.org/letswave>). First, we applied a 0.3-30 Hz bandpass filter to the continuous EEG data (zero-phase Butterworth filter). The EEG was then segmented into epochs extending from -500 to +1000 ms after the stimulus onset. Artefacts due to blinking or eye movements were then removed using a validated method based on independent component analysis (FastICA algorithm) [15]. Epochs with amplitude values exceeding $\pm 100 \mu\text{V}$ were rejected. After baseline correction (reference interval: -500 to 0 ms), the data were re-referenced to Fz (in different datasets). Separate average waveforms were computed for each participant and for the different stimulation sites.

Source modelling

Dipolar source modelling was performed using Brain Electrical Source Analysis (BESA, BESA Research, MEGIS GmbH, Gräfelfing, Germany). This tool, using surface-recorded EEG, estimates the source activities generating the topography of the scalp-evoked potentials. BESA calculates the surface potential topography from fixed dipoles within the brain. Then, it compares the recorded potential distribution with the calculated one and the percentage of the recorded signal that cannot be explained by the dipole model represents the residual variance. Using an algorithm based on repetitive iterations, BESA calculates a hypothetical model that does not rule out other possible solutions. The validity of the model is underpinned by its applicability to individual data and consistency with the anatomical and physiological knowledge of the identified source areas. The latency interval between 100 ms and 400 ms, including all the reliable CEP components in all our subjects, was analysed. Dipoles were fitted using a sequential strategy, as detailed in previous studies [35-37]. When calculating the dipole model, we verified that up to 5 dipoles could be activated together so that the independent dipolar parameters (six per dipole) did not exceed the number of recording electrodes [37]. In order to build the dipole models, grand averages of the CEPs from stimulating both the supraorbital and perioral regions were obtained across all our subjects. We initially analysed the grand averages, then applied the calculated models to all individual subjects.

Diagnostic procedures in patients

The two patients underwent precise sensory profiling using bedside tools and quantitative sensory testing to assess thermal-pain perceptual thresholds (ATS, PATHWAY, Medoc, Israel). Following the previously described methodological procedures both patients underwent cold and laser stimulation of the perioral regions. In the patient with trigeminal neuropathy, we also recorded laser

evoked potentials related to C-fibre activation. In this patient, we used laser pulses of low intensity (46 mJ/mm^2), relatively-long duration (10 ms) and large diameter ($\sim 10 \text{ mm}$), eliciting purely warm sensations related to C-fibre input [32]. The patient with trigeminal neuropathy also underwent a skin biopsy of the supraorbital region. A two-mm punch skin biopsy was taken immediately above the eyebrow. The wound healed in a few days without a visible scar. The skin sample was processed using immunohistochemical techniques and epidermal and dermal nerve fibre density was assessed as previously described [34].

Statistical analysis

We used Graphpad, Version 8 for the statistical analysis. All the data had normal distributions, as assessed using the D'Agostino & Pearson normality test. We used the One-Way ANOVA with the Greenhouse-Geisser correction and Tukey's multiple comparisons test to assess the differences in cold and laser evoked potential variables across the three stimulation sites (supraorbital, perioral and hand). To test the differences between cold and laser evoked potential variables after supraorbital and perioral stimulation, we used the paired t-test and applied the Bonferroni correction. To estimate conduction velocity, we calculated $1/\text{slope}$ of the regression line for the N2 latencies obtained at the three stimulation sites (hand, forearm and shoulder). The $p < 0.05$ level was considered statistically significant.

Results

Psychometric measures

Cold stimulation at 10°C evoked a painless cold sensation in all healthy participants. The mean intensity of the cold sensation did not differ across the three stimulation areas (4.5 ± 1.2 after

supraorbital stimulation, 5.0 ± 1.3 after perioral stimulation and 4.9 ± 1.1 after hand stimulation, $p=0.4$, $F:0.7573$, GG epsilon:0.9782, DF:2).

In all healthy participants, laser stimuli (intensity 64-140 mJ/mm²) evoked a clear painful pinprick sensation. The mean intensity of the painful pinprick sensation (4.7 ± 1.5 after supraorbital stimulation, 5.7 ± 1.2 after perioral stimulation and 4.4 ± 1.1 after hand stimulation) was significantly higher after the perioral stimulation than the supraorbital and hand stimulation ($p=0.001$, $F:11.19$, GG epsilon:0.7838, DF:2).

Scalp potentials in healthy participants

We excluded one subject due to technical difficulties during scalp recordings.

The CEPs consisted of a biphasic negative-positive complex (N2-P2), with maximum amplitude at the vertex (Cz). The mean frequency of identifiable N2 responses (defined as a 2.5 fold increase from the baseline noise level) across participants was 64.5%, 63.5%, 55.0% after supraorbital, perioral and hand stimulation. The mean frequency of identifiable P2 responses (defined as a 2.5 fold increase from the baseline noise level) was 71.8%, 73.1% and 79.2% after supraorbital, perioral and hand stimulation. This N2-P2 vertex complex was preceded by a negative component (N1) over the contralateral temporal areas. ANOVA analysis using Tukey's multiple comparison test showed that supraorbital and perioral cold stimulation yielded scalp potentials of similar latency and amplitude. Hand dorsum stimulation elicited CEPs with longer latency but similar amplitude than supraorbital and perioral stimulation (latency N1: $p<0.001$, $F:13.59$, GG epsilon:0.6608, DF: 2; amplitude N1: $p=0.4$, $F:0.7913$, GG epsilon:0.8925, DF: 2; latency N2: $p<0.001$, $F:22.94$, GG epsilon:0.6144, DF:2; amplitude N2-P2: $p=0.3$, $F: 1.423$, GG epsilon:0.9108, DF: 2) (Figure 1).

The regression line, calculated from the N2-wave latencies from the three stimulation sites, indicated a significant linear relationship between distance and time (R square: 0.421; F: 7.248; $p=0.02$; Figure 2). The resulting conduction velocity (reciprocal of the slope) was 12.7 m/s.

Laser stimulation of the supraorbital and perioral regions evoked a large vertex complex (N2-P2), preceded by a far smaller negativity (N1) over contralateral temporal areas. The latency of LEPs was earlier and the amplitude larger after perioral than supraorbital and hand dorsum stimulation (N1 latency: $p<0.001$, F:41.49, GG epsilon:0.5248, DF:2; N1 amplitude: $p=0.06$, F:3.425, GG epsilon:0.8312, DF:2; N2 latency: $p<0.001$, F:65.57, GG epsilon:0.6428, DF:2; N2-P2 amplitude: $p<0.001$, F:25.12, GG epsilon:0.9013, DF:2) (Figure 1).

The latency of the scalp potentials evoked by cold stimulation was about 30 ms longer than that evoked by laser stimuli ($p<0.01$, by paired t-test). The amplitude of the N2-P2 complex evoked by cold stimuli was lower than that evoked by laser stimulation ($p<0.01$, by paired t-test). Conversely, the N1 amplitude did not differ between the two types of stimulation (Table 1) (supplementary figure 1, available at <http://links.lww.com/PAIN/A783>).

Dipolar source analysis

The dipole models calculated from the grand-average CEPs after supraorbital and perioral stimulation were virtually identical. The scalp topography between 100 ms and 160 ms was analysed and explained by a bilateral opercular source (Figure 3). The modelled interval was then prolonged up to 400 ms and 3 other sources had to be added. After fitting, one source reached a midline position, possibly corresponding to the cingulate cortex, while the remaining 2 dipoles showed a very superficial, almost symmetrical, position in the dorso-lateral frontal cortex. The residual variance for the CEPs models after supraorbital and perioral stimulation were 7.6% and 8.7%, respectively. The next step was to apply the grand average models to individual traces. In

order to do so, dipole coordinates (x, y and z) and orientations were let free to change. The residual variance of the individual models was lower than 10% in 5 and 3 subjects for CEPs from supraorbital and perioral stimulation, respectively (Table 2).

Patients

In patient 1, clinical and quantitative sensory testing showed a severe deficit in tactile and cold sensation (cold detection threshold: 21.9°C), while the pinprick sensation was only mildly affected and the warm sensation spared (warm detection threshold: 34.6 °C) (supplementary figure 2, available at <http://links.lww.com/PAIN/A783>). Accordingly, laser evoked potentials related to nociceptive A δ -fibres had a reduced amplitude and delayed latency and laser evoked potentials related to C-fibres were spared. Cold stimulation failed to evoke scalp potentials. In this patient skin biopsy showed normal epidermal unmyelinated nerve fibre and reduced dermal myelinated nerve fibre density (Figure 4).

In patient 2, clinical and quantitative sensory testing showed severe cold allodynia (cold pain threshold: 25.3°C; cold detection threshold: 26.9°C). Conversely, warm sensation was only mildly abnormal (warm detection threshold: 36.8°C) (supplementary figure 2, available at <http://links.lww.com/PAIN/A783>). Laser stimulation of the affected side evoked dampened, though still preserved, scalp potentials. Conversely, cold stimulation failed to evoke scalp potentials after stimulating the affected side (Figure 5).

Discussion

In this clinical and neurophysiological study, we showed that in healthy participants this new tool evokes reproducible scalp potentials related to cold-mediating fibres. Dipolar source analysis showed that the scalp CEP generators included the opercular cortex, dorso-lateral frontal region and the anterior cingulate cortex. In the two patients with exemplary trigeminal neuropathic pain conditions, CEP recording provided distinct information on cold-mediating fibre damage.

Psychometric measures and scalp potentials in healthy participants

We used a new cold stimulator, capable of achieving very steep cooling ramps up to -300°C/s . As shown in a recent study, this new device yields different stimulation surfaces (40-120 mm²) and different target temperature [6]. We used 10°C as the target temperature and the maximum stimulating area (120 mm²), given that the study by De Keyser et al. showed that CEP amplitude is influenced by the stimulation area (the larger the stimulation area, the larger the CEP amplitude).

In all healthy participants, 10°C stimuli evoked a distinct, painless cold sensation. No subject reported painful sensations after cold stimulation, despite the low target temperature, probably due to the phasic and short duration of the stimulus. Unexpectedly, the magnitude of the cold sensation and the amplitude of CEPs did not differ across the various stimulation sites, including the hand. Conversely, laser stimulation of the perioral regions yielded a higher rating for pinprick sensation and larger amplitude scalp potentials than supraorbital and hand stimulation, probably due to the higher density of mechano-heat receptors [27]. This lack of differences in the cold sensation and CEP amplitude across the different stimulation sites, though compatible with previous studies investigating warm sensation [33], is not in line with previous studies showing that temperature sensitivity is not evenly distributed over the surface of the body [30].

The conduction velocity of cold-mediating fibres we measured (12.7 m/s) is compatible with small myelinated A δ -fibre activation. Human and animal studies have shown that cold-mediating A δ -fibres have a conduction velocity of 9-15 m/s [5,8,17]. Laser evoked potentials are similarly mediated by A δ -fibres (though related to mechano-heat receptors) with a relatively similar conduction velocity [31]. However, in our study the CEP latency is about 20-30 ms longer than that of laser evoked potentials. We cannot rule out that this latency difference reflects a different central nervous system processing of cold afferent input. We speculate, however, that the long latency of CEPs probably depends on the longer duration of cold stimulus rather than laser stimulation (500 ms for the cold stimulation and 5 ms for laser stimulation) and the different amount of time required for the temperature change (conduction for the cold and radiation for the laser stimulation).

The amplitude of the N1 component of CEPs was similar to that of laser evoked potentials. Conversely, the amplitude of the N2-P2 vertex complex was smaller after cold than laser stimulation. Whereas the lateralized N1 component predominantly reflects the sensory discriminative component of the somatosensory afferent input [12, 26], the N2-P2 complex is not merely related to the somatosensory afferent input; it also reflects neural activities involved in stimulus-triggered mechanisms of arousal or attentional capture [21]. Accordingly, stimulus saliency strongly influences the magnitude of the N2-P2 complex [16]. In our study, although laser stimulation invariably evoked a painful pinprick sensation, cold stimulation evoked a painless cold sensation in all healthy participants. Hence, the lower amplitude of CEPs than that of laser evoked potentials probably depends on the low saliency of non-painful cold stimulation.

We found that in our healthy participants trigeminal CEPs have shorter latency and larger amplitude than those reported in a recent study [14]. The difference is probably due to technical reasons. Hüllemann and colleagues investigated trigeminal CEPs by cooling the skin from 30 to 25°C in approximately 0.5 s, i.e. using a cooling rate of -10°C/s. Conversely, we used a 10° target temperature with a cooling rate of 300°C/s. The steeper cooling rate and the higher stimulus

intensity we used in our study compared to those used in the Hüllemann et al. study probably explain the differences in CEP measures.

Dipolar source analysis

Dipolar modelling showed that the CEP wave generators included three brain regions, namely the opercular cortex, the dorso-lateral frontal region and the anterior cingulate.

The role of the opercular cortex as a CEP generator is supported by several studies. EEG studies in healthy humans and patients have shown that non-painful cold stimulation evokes responses in the perisylvian regions [10, 13]. A recent MRI study in humans showed that the parietal-opercular (SII) cortex is primarily implicated in thermosensory processing [23]. Therefore, the early activation of the bilateral opercular source in our subjects suggests that the SII area and/or the insula may be important in cold discrimination, with a role similar to the one played by the opercular cortex in pain perception [11].

Although the functional meaning of the bilateral frontal dipole is difficult to explain, previous studies partly support the involvement of frontal areas in cold perception. The results of EEG power analysis during painful cold stimulation in healthy humans support the involvement of the frontal lobe in cold perception [22, 29]. Primary motor cortex inhibition, obtained using cathodal transcranial direct current stimulation, increases the non-painful cold perception threshold [1]. Interestingly, a recent fMRI study showed that bilateral frontal areas are activated during cold allodynia, but not during warm stimulation [9]. Admittedly, BESA spatial resolution does not identify frontal dipole topography with extreme accuracy. Therefore, we cannot rule out that these frontal dipoles correspond to perirolandic region activation.

The fact that the anterior cingulate cortex is one of the scalp CEP generators is not surprising. This brain region processes stimuli of different modalities and is involved in many different cognitive tasks [20,39].

Findings in patients

Patient 1 suffered from idiopathic trigeminal neuropathy manifesting with pain and consisting in dissociated nerve-fibre damage predominantly affecting trigeminal large myelinated fibres and sparing the unmyelinated fibres. Previous observations showed that in patients with idiopathic trigeminal neuropathy the larger the diameter of the myelinated fibre, the more severe the axonal loss [4]. Accordingly, we found that cold stimulation failed to evoke reproducible A δ -fibre mediated CEPs. Conversely, the A δ -fibre mediated laser evoked potentials, although of low amplitude and delayed latency, were still preserved. The dissociation between cold and mechano-heat fibres we found is in line with human experimental studies using the mechanical block of peripheral nerves. These studies showed that, during mechanical block the sensations of cold and touch disappear almost simultaneously, while the pinprick sensation evoked by laser stimuli disappears over a longer period of time [24]. These experimental observations indicate that the myelinated A δ -fibres mediating cold sensation are larger than the myelinated A δ -fibres mediating mechano-heat sensations [25]. In this patient, we found that C-fibre mediated laser evoked potentials were spared. Accordingly, skin biopsy data showing the sparing of unmyelinated epidermal nerve fibres and the loss of myelinated dermal nerve fibres were in line with neurophysiological findings. C-fibre sparing in this patient with painful neuropathy argues against classic notions about ongoing pain, postulating that this type of pain is associated with C-fibre damage [4]. A possible explanation for these contrasting results on the relationship between myelinated nerve fibre damage, unmyelinated fibre sparing and the development of neuropathic

pain may lie in the imbalanced input from myelinated and unmyelinated nerve fibres onto the second-order neuron [4].

Patient 2 suffered from central post-stroke pain. The clinical examination and quantitative sensory testing showed dissociated sensory loss, mostly affecting cold sensation. Accordingly, we found absent CEPs and partially spared laser evoked potentials. These findings are in line with many studies reporting that neuropathic pain due to thalamic lesion is commonly associated with predominant cold system damage [18, 19]. Previous studies have suggested that the imbalance between cold-afferent pathways and thermal-pain pathways [3] is probably responsible for central post-stroke pain due to thalamic lesions.

Conclusions

Our clinical and neurophysiological study has shown that in healthy participants this new cold stimulator evokes reproducible scalp potentials and in patients with exemplary trigeminal neuropathic pain conditions provides distinct information on cold-mediating fibre damage. Therefore, we believe that CEPs might be a reliable tool for investigating neuropathic pain and dissociated small-fibre damage for clinical and experimental purposes.

Disclosures: Dr Dufour has a pending patent for the cold stimulator. The other Authors have no conflict of interest to declare.

References

1. Bachmann CG, Muschinsky S, Nitsche MA, Rolke R, Magerl W, Treede RD, Paulus W, Happe S. Transcranial direct current stimulation of the motor cortex induces distinct changes in thermal and mechanical sensory percepts. *Clin Neurophysiol* 2010;121(12):2083-9
2. Baumgärtner U, Greffrath W, Treede RD. Contact heat and cold, mechanical, electrical and chemical stimuli to elicit small fiber-evoked potentials: merits and limitations for basic science and clinical use. *Neurophysiol Clin* 2012;42(5):267-80.
3. Craig AD. A new version of the thalamic disinhibition hypothesis of central pain. *Pain Forum* 1998; 7: 1–14.
4. Cruccu G, Pennisi EM, Antonini G, Biasiotta A, di Stefano G, La Cesa S, Leone C, Raffa S, Sommer C, Truini A. Trigeminal isolated sensory neuropathy (TISN) and FOSMN syndrome: despite a dissimilar disease course do they share common pathophysiological mechanisms? *BMC Neurol* 2014;14:248
5. Darian-Smith I, Johnson KO, Dykes R. "Cold" fiber population innervating palmar and digital skin of the monkey: responses to cooling pulses. *J Neurophysiol* 1973;36(2):325-46.
6. De Keyser R, van den Broeke EN, Courtin A, Dufour A, Mouraux A. Event-related brain potentials elicited by high-speed cooling of the skin: A robust and non-painful method to assess the spinothalamic system in humans. *Clin Neurophysiol* 2018;129(5):1011-1019
7. Di Stefano G, La Cesa S, Leone C, Pepe A, Galosi E, Fiorelli M, Valeriani M, Lacerenza M, Pergolini M, Biasiotta A, Cruccu G, Truini A. Diagnostic accuracy of laser-evoked potentials in diabetic neuropathy. *Pain* 2017;158(6):1100-1107.

8. Dubner R, Sumino R, Wood WL. A peripheral "cold" fiber population responsive to innocuous and noxious thermal stimuli applied to monkey's face. *J Neurophysiol* 1975;38(6):1373-89.
9. Eisenblätter A, Lewis R, Dörfler A, Forster C, Zimmermann K. Brain mechanisms of abnormal temperature perception in cold allodynia induced by ciguatoxin. *Ann Neurol* 2017;81(1):104-116
10. Fardo F, Vinding MC, Allen M, Jensen TS, Finnerup NB. Delta and gamma oscillations in operculo-insular cortex underlie innocuous cold thermosensation. *J Neurophysiol* 2017;117(5):1959-1968.
11. Garcia-Larrea L. The posterior insular-opercular region and the search of a primary cortex for pain. *Neurophysiol Clin* 2012;42(5):299-313
12. Garcia-Larrea L, Peyron R. Pain matrices and neuropathic pain matrices: a review. *Pain* 2013;154 Suppl 1: S29-4
13. Greenspan JD, Ohara S, Franaszczuk P, Veldhuijzen DS, Lenz FA. Cold stimuli evoke potentials that can be recorded directly from parasympathetic cortex in humans. *J Neurophysiol* 2008;100(4):2282-6.
14. Hüllemann P, Nerdal A, Binder A, Helfert S, Reimer M, Baron R. Cold-evoked potentials - Ready for clinical use? *Eur J Pain* 2016;20(10):1730-1740.
15. Hyvärinen A, Oja E. Independent component analysis: algorithms and applications. *Neural Netw* 2000; 13(4-5):411-30.
16. Iannetti GD, Hughes NP, Lee MC, Mouraux A. Determinants of laser-evoked EEG responses: pain perception or stimulus saliency? *J Neurophysiol* 2008 Aug;100(2):815-28.
17. Kenshalo DR, Duclaux R. Response characteristics of cutaneous cold receptors in the monkey. *J Neurophysiol* 1977;40(2):319-32.

18. Kim JH, Greenspan JD, Coghill RC, Ohara S, Lenz FA. Lesions Limited to the Human Thalamic Principal Somatosensory Nucleus (Ventral Caudal) Are Associated with Loss of Cold Sensations and Central Pain. *The Journal of Neuroscience* 2007;27(18):4995–5005
19. Klit H et al. Central post-stroke pain: clinical characteristics, pathophysiology, and management. *Lancet Neurol* 2009; 8: 857–68
20. Kolling N, Behrens T, Wittmann MK, Rushworth M. Multiple signals in anterior cingulate cortex. *Curr Opin Neurobiol* 2016;37:36-43
21. La Cesa S, Di Stefano G, Leone C, Pepe A, Galosi E, Alu F, Fasolino A, Cruccu G, Valeriani M, Truini A. Skin denervation does not alter cortical potentials to surface concentric electrode stimulation: A comparison with laser evoked potentials and contact heat evoked potentials. *Eur J Pain* 2018;22(1):161-169.
22. Levitt J, Choo HJ, Smith KA, LeBlanc BW, Saab CY. Electroencephalographic frontal synchrony and caudal asynchrony during painful hand immersion in cold water. *Brain Res Bull* 2017;130:75-80
23. Mano H, Yoshida W, Shibata K, Zhang S, Koltzenburg M, Kawato M, Seymour B.J Thermosensory Perceptual Learning Is Associated with Structural Brain Changes in Parietal-Opercular(SII) Cortex. *Neurosci* 2017;37(39):9380-9388
24. Nahra H, Plaghki L. The effects of A-fiber pressure block on perception and neurophysiological correlates of brief non-painful and painful CO2 laser stimuli in humans. *Eur J Pain* 2003;7(2):189-99.
25. Ochoa J et al. Anatomical changes in peripheral nerves compressed by a pneumatic tourniquet. *J Anat* 1972;113(Pt 3):433-55.
26. Perchet C, Godinho F, Mazza S, Frot M, Legrain V, Magnin M, Garcia-Larrea L. Evoked potentials to nociceptive stimuli delivered by CO2 or Nd:YAP lasers. *Clin Neurophysiol* 2008;119(11):2615-22.

27. Romaniello A, Iannetti GD, Truini A, Cruccu G. Trigeminal responses to laser stimuli. *Neurophysiol Clin* 2003; 33:315–24.
28. Rosner J, Rinert J, Ernst M, Curt A, Hubli M. Cold evoked potentials: Acquisition from cervical dermatomes. *Neurophysiol Clin* 2019;49(1):49-57.
29. Shao S, Shen K, Yu K, Wilder-Smith EP, Li X. Frequency-domain EEG source analysis for acute tonic cold pain perception. *Clin Neurophysiol* 2012;123(10):2042-9.
30. Stevens JC, Choo KK. Temperature sensitivity of the body surface over the life span. *Somatosens Mot Res.* 1998;15(1):13-28.
31. Treede RD, Meyer RA, Raja SN, Campbell JN. Evidence for two different heat transduction mechanisms in nociceptive primary afferents innervating monkey skin. *J Physiol* 1995;483 (Pt 3):747-58.
32. Truini A, Galeotti F, Pennisi E, Casa F, Biasiotta A, Cruccu G. Trigeminal small-fibre function assessed with contact heat evoked potentials in humans. *Pain* 2007;132(1-2):102-7.
33. Truini A, Leone C, Di Stefano G, Biasiotta A, La Cesa S, Teofoli P, Padua L, Cruccu G. Topographical distribution of warmth, burning and itch sensations in healthy humans. *Neurosci Lett* 2011;494(2):165-8.
34. Truini A, Haanpaa M, Provitera V, Biasiotta A, Stancanelli A, Caporaso G, Santoro L, Cruccu G, Nolano M. Differential myelinated and unmyelinated sensory and autonomic skin nerve fiber involvement in patients with ophthalmic postherpetic neuralgia. *Front Neuroanat* 2015 4;9:
35. Valeriani M, Rambaud L, Mauguière F. Scalp topography and dipolar source modelling of potentials evoked by CO2 laser stimulation of the hand. *Electroencephalogr Clin Neurophysiol* 1996;100(4):343-53.
36. Valeriani M, Restuccia D, Di Lazzaro V, Le Pera D, Tonali P. The pathophysiology of giant SEPs in cortical myoclonus: a scalp topography and dipolar source modelling study. *Electroencephalogr Clin Neurophysiol* 1997;104(2):122-31

37. Valeriani M, Le Pera D, Tonali P. Characterizing somatosensory evoked potential sources with dipole models: advantages and limitations. *Muscle Nerve* 2001;24(3):325-39
38. Valeriani M, Pazzaglia C, Cruccu G, Truini A. Clinical usefulness of laser evoked potentials. *Neurophysiol Clin* 2012 Oct;42(5):345-53.
39. Vogt BA. Midcingulate cortex: Structure, connections, homologies, functions and diseases. *J Chem Neuroanat* 2016 Jul; 74:28-46

Legends to Figures

Figure 1. Evoked potential recording. Vertex complex (N2-P2 recorded at Cz-A1) and lateralized component (N1, recorded at Tc-Fz) of cold evoked potentials (blue traces) and laser evoked potentials (red traces) after supraorbital, perioral and hand stimulation. Each trace represents the grand-average for each stimulus condition. Dotted lines indicate the stimulus onset.

Figure 2. Peripheral conduction velocity of the cold-mediating fibres. The dashed lines represent the regressions of individual latencies in five subjects. The thin line corresponds to the mean regression. Dots represent mean and standard deviation of the N2 components after stimulation of the three sites. Y-axis: N2 latency. The reciprocal of the slope of the mean regression (12.7 m/s) indicates the mean conduction velocity.

Figure 3. Dipolar modelling of cold evoked potentials. Dipole sources projected on a MRI model. R and L correspond to right and left side, respectively. The opercular dipoles (blue and red), the cingulate source (green), and the dorso-lateral frontal dipoles (purple and brown) are shown.

Figure 4. Neurophysiological and skin biopsy findings in the patient with idiopathic

trigeminal neuropathy. A, B: Vertex complex of A δ - and C-fibre mediated laser evoked potentials (LEP, red traces) after stimulation of the perioral region; C: Vertex complex of cold evoked potentials (CEP, blue traces) after stimulation of the perioral region. Each trace represents the average of 20 trials. Dotted lines indicate the stimulus onset. Whereas cold evoked potentials related to A δ -fibres were absent, laser evoked potentials related to A δ -fibres were partially preserved and those related to C-fibre spared. The skin biopsy of the perioral region showed a predominantly involvement of myelinated fibres along with the sparing of unmyelinated fibres. Confocal images of facial innervation in the patient with trigeminal neuropathy (D, E) compared to a healthy control (F, G) showing a normal distribution of epidermal nerve fibres (D compared to F). contrasting with the severe loss of myelinated fibres (E compared to G). Scale bar 100 micron in D and F, 200 micron in E and G.

Figure 5. Neurophysiological and MRI findings in the patient with central post-stroke pain.

Vertex complex (N2-P2 recorded at Cz-A1) of cold evoked potentials (CEP, blue traces) and laser evoked potentials (LEP, red traces) after stimulation of the healthy and the affected side. Each trace represents the average of 20-30 trials. Dotted lines indicate the stimulus onset. Whereas the laser stimulation of the affected side yielded dampened, though still present, scalp potentials, cold stimulation failed to evoke reproducible scalp potentials. MRI images showed a right thalamic posterior lesion.

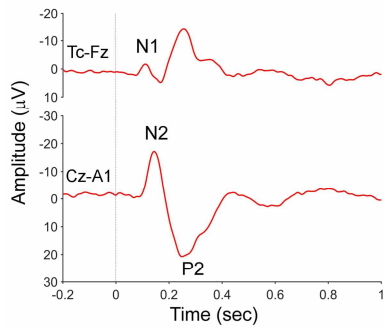
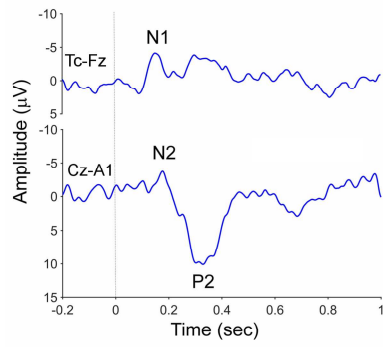
Table 1. Comparison between cold and laser evoked potentials variables

	Supraorbital region			Perioral region			Hand dorsum		
	Cold stimulation	Laser stimulation	p*	Cold stimulation	Laser stimulation	p*	Cold stimulation	Laser stimulation	p*
N1 latency (ms)	142.4±8.3	114.1±13.9	<0.01	139.1±18.9	107.4±15.2	<0.01	180.9±36.3	164±8.9	<0.01
N1 amplitude (µV)	5.0±2.3	5.3±4.0	0.8	6.3±3.5	9.0±6.5	0.2	6.3±3.9	6.5±3.3	0.3
N2 Latency (ms)	176±17.04	148.1±12.1	<0.01	173.6±26.4	139.4±14.9	0.002	227.3±33.6	199±10.9	<0.01
P2 latency (ms)	302.1±46.3	247.0±15.3	<0.01	289.0±49.5	243.5±18.8	<0.01	353.6±40.9	296.2±15.9	<0.01
N2-P2 amplitude (µV)	16.9±4.6	39.1±13.6	<0.01	18.2±4.9	51.2±16.8	<0.01	20.1±6.8	30.5±7.5	<0.01
* paired t-test; p after Bonferroni correction									

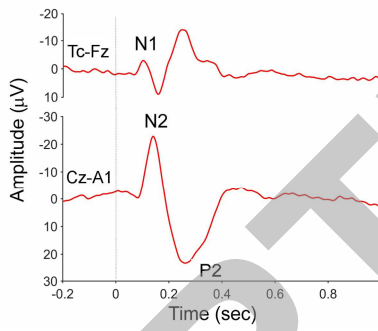
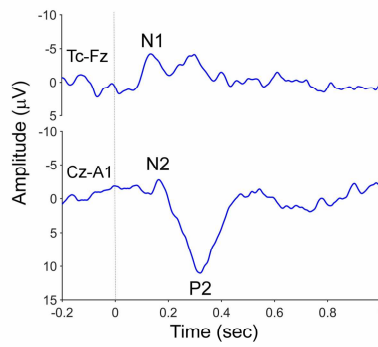
Table 2: Talairach's coordinates of the dipolar sources

Source	Supraorbital stimulation			Perioral stimulation		
	x	y	z	x	y	z
Left opercular	-57.6±3.9	-16.4±10.2	31.6±10.2	-54.1±7	-14±5.2	30.±7.5
Right opercular	57.8±9.3	-17.9±9.6	19.7±4.2	66.6±4.4	-16±5.1	19.3±4.2
Anterior cingulate	10.2±6	2.1±5.8	47.4±6.1	9.2±4.3	-0.5±7.4	46±4.7
Left frontal	-48.5±6.7	-15.1±3.8	63.2±1.7	-49.7±3.3	-16.4±4.4	63.7±3.7
Right frontal	41.6±3.5	-0.7±3.3	68±1.7	36.5±1.5	-0.5±8.4	71.4±5.6

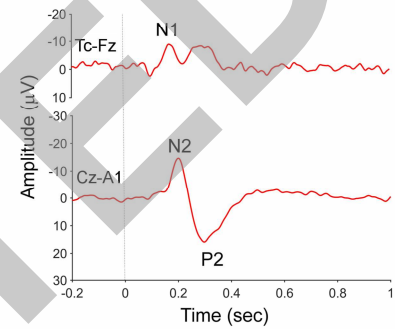
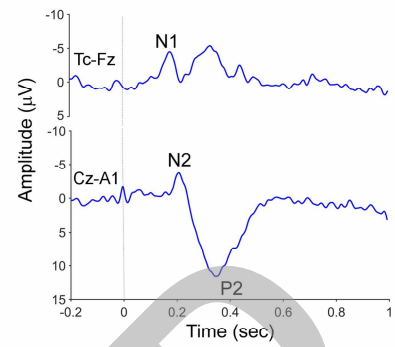
Supraorbital stimulation

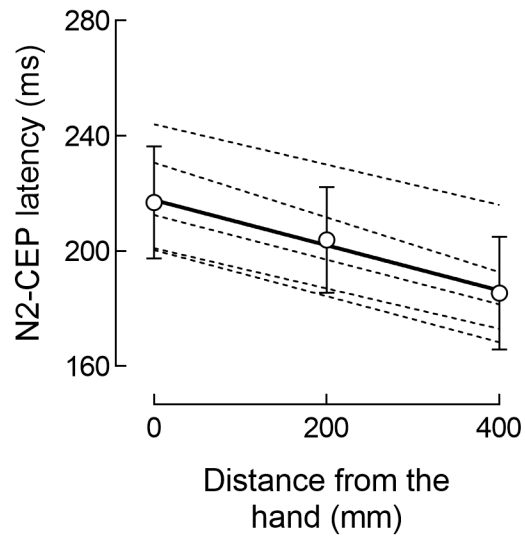


Perioral stimulation

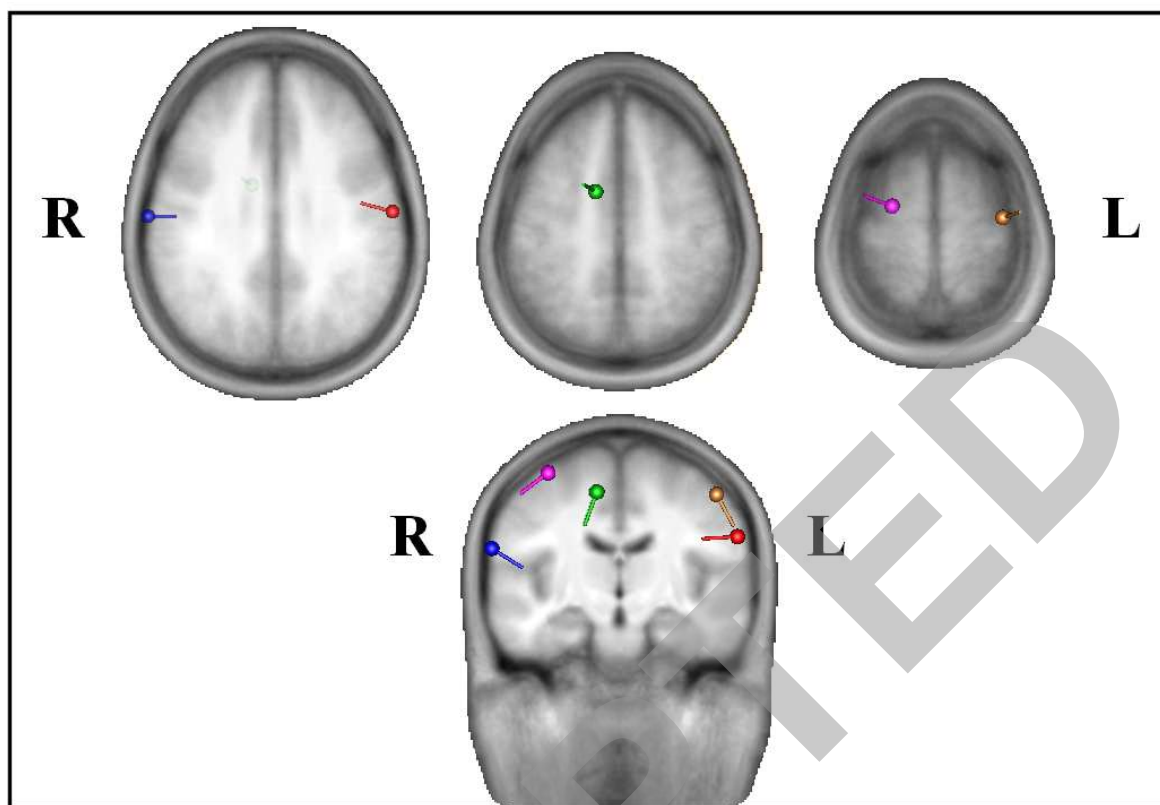


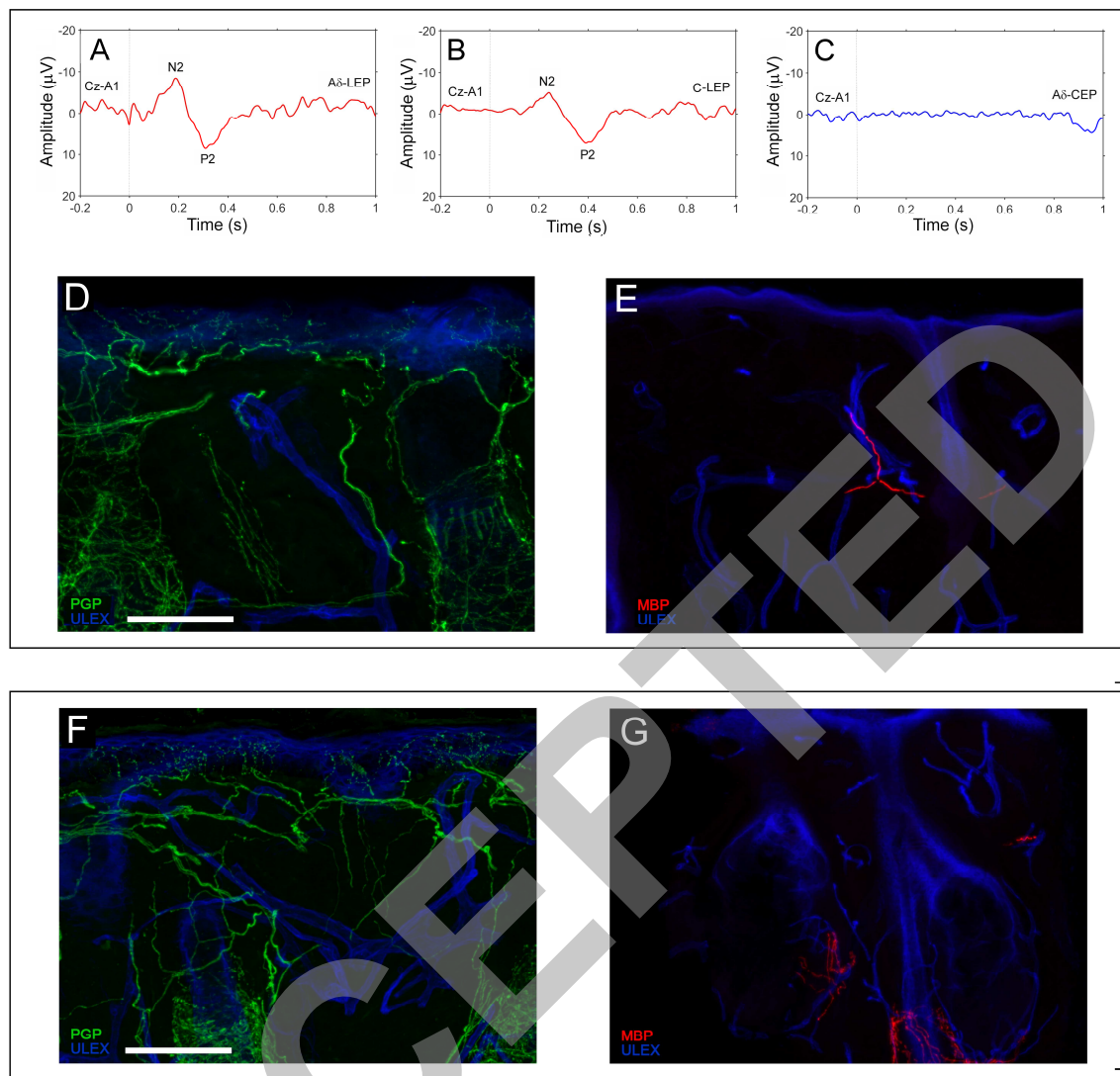
Hand stimulation

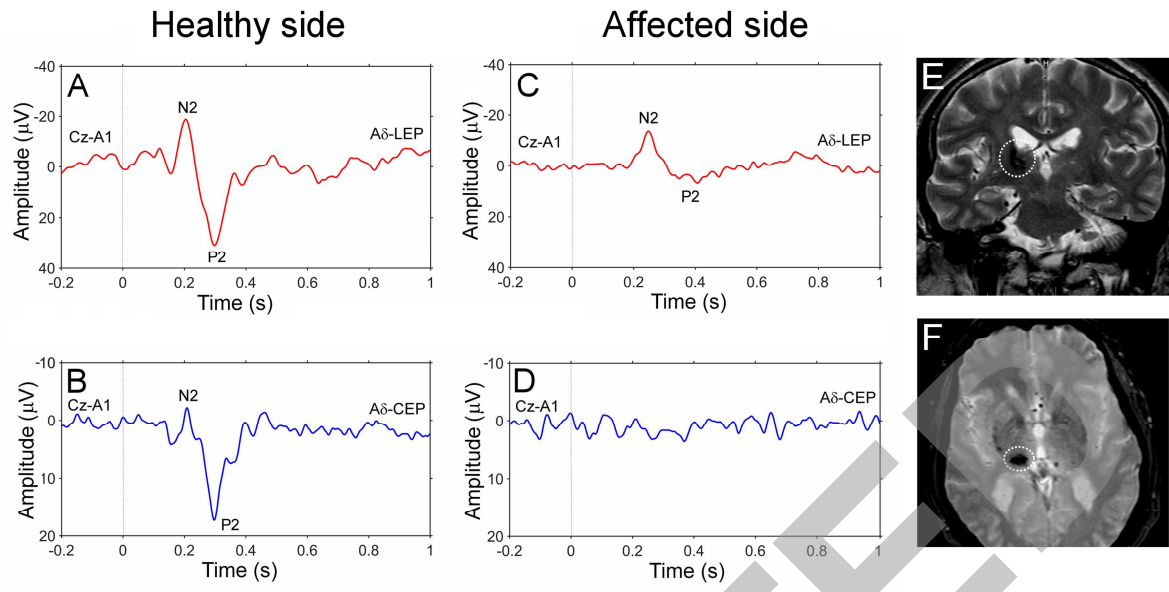


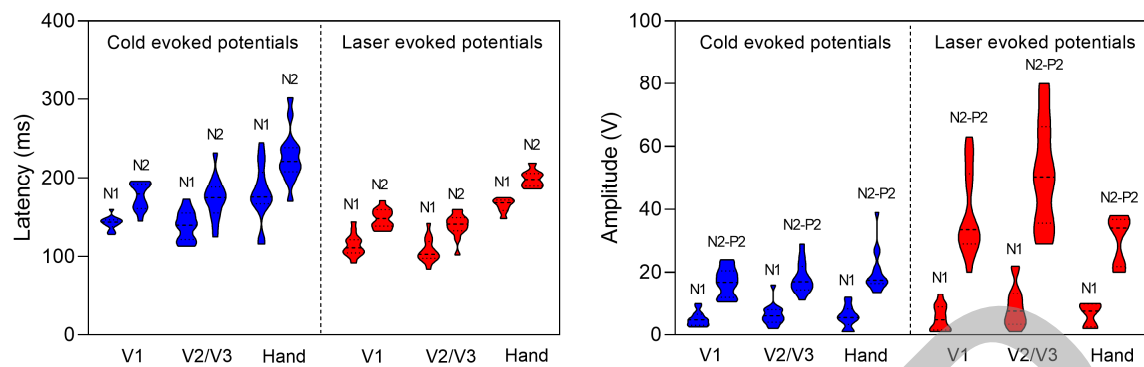


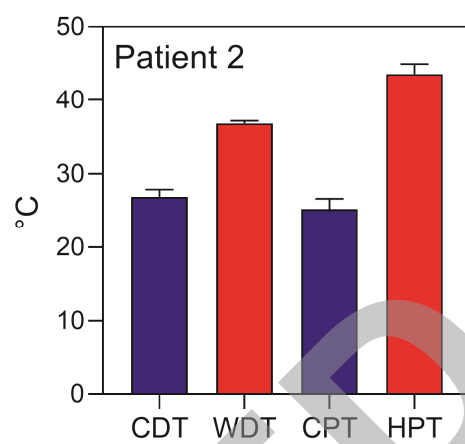
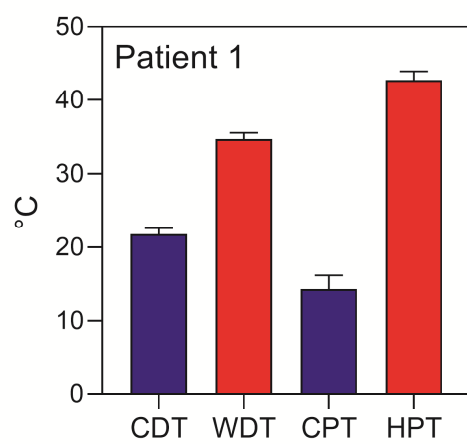
ACCEPTED











ACCEPTED